Journal of Materials Chemistry A

Accepted Manuscript

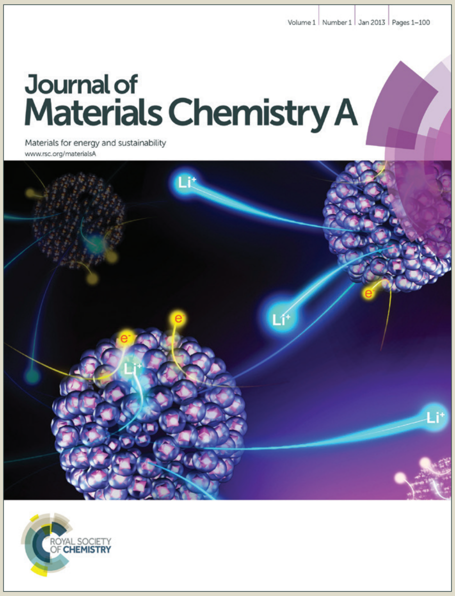

ROYAL SOCIETY OF CHEMISTRY

www.rsc.org/materialsA

Facile Removal of Polyvinylpyrrolidone (PVP) Adsorbates from Pt Alloy Nanoparticles

Muhua Luo, [1] **Yuanchen Hong,** [1] **Weifeng YAO,** [1*] **Cunping Huang,** [2] **Qunjie Xu,**[1] **Qiang Wu**[1]

[1] **College of Environmental & Chemical Engineering, Shanghai University of Electric Power, Shanghai, P. R. China.** [2]**Aviation Research Division, Federal Aviation Administration William J. Hughes Technical Center, Atlantic City International Airport, NJ 08405**

Abstract

The synthesis of colloidal Pt and Pt alloy nanoparticles (NPs) requires surfactants and capping agents to inhibit the overgrowth and aggregation of NPs. These reagents are also needed in the shape control synthesis of NPs to vary crystal growth rates in selected directions. Polyvinylpyrrolidone (PVP) is one of the most common water soluble capping agents for use in the synthesis of colloidal particles. However, PVP strongly adsorbed onto the surface of nanoparticles is detrimental when the NPs are used as catalysts, because surface adsorbed PVP blocks the access of reactant molecules to the active sites of nanoparticles. In this paper, we report a facile $NaBH_4$/tert-butylamine (TBA) treatment technology for the effective removal of PVP from the surface of colloidal Pt-Pd nanocubes (NCs). The method does not change the morphology of the NPs. After treatment, catalytic activity of Pt-Pd NCs has been significantly improved due to greater particle surface areas available for catalytic reactions. This facile method will find extensive applications in the fields of fuel cells, water electrolysis and photocatalytic hydrogen production.

1. Introduction

Pt and Pt alloy nanoparticles (NPs) are fundamental catalysts widely used in fuel cells,[1] water electrolysis [2, 3] and photocatalysis for hydrogen production.[4] Due to its high cost and limited reserves it is urgent to reduce the amount of Pt usage. Using Pt alloy NPs to replace pure Pt NPs is one of the effective and most studied approaches for the reduction of Pt consumption.[5-7] Not only can Pt alloy NPS retain the properties of pure Pt NPs, but they can also exhibit superior activities in comparison to monometallic Pt NPs. Recently, the shape controlled synthesis of Pt alloy NPs has attracted more research attention because of their enhanced catalytic activity and selectivity for a variety of catalytic reactions. The essence of the shape effect of Pt alloy NPs is the exposure of more effective crystal planes to reactant molecules.[2, 3, 8-11]

Commonly, colloidal Pt alloy NPs are synthesized and stabilized in an aqueous solution in the presence of surfactants and/or capping agents, such as oleylamine, oleic acid and polyvinylpyrrolidone (PVP), which can bind onto the particle surfaces and protect them from aggregation. In promoting the growth of highly active crystal planes of NPs, stronger adsorption of a capping agent on the surface of the NPs is critical. However, when a higher strength capping agent is used its removal from the surface of NPs requires greater efforts when the NPs are used as catalysts. This is due to the fact that the existence of strongly adsorbed capping agents can block the access of reactant molecules to the surface atoms, thereby lowering activity of the NPs.[12, 13] It is, therefore, critical to develop efficient methods for the removal of capping agents from NPs without significantly changing the shape and size of synthesized NPs.

Although excess capping agents could be stripped from the surface of NPs by extensive washing, low concentrations of capping agents strongly adsorbed onto the surface of NPs are difficult to remove. To date, the most established method is the heat-treatment of stabilized NPs in an oxidizing atmosphere, followed by intensive washing. For example, in order to remove PVP, Pt cubic particles must be heated to PVP decomposition temperature (473 - 623 K) in a 20% O_2/He atmosphere.[14] However, in this temperature range, particle agglomeration and shape change cannot be avoided.[15] The heating temperature needed for removing capping agents is also affected by supporting materials of Pt NPs.[16, 17] In order to avoid high temperature treatment, Pt NPs can be exposed to UV light irradiation under an ozone atmosphere (UV-O_3 technology), a strong oxidizing agent.[18] In this case, although the morphology of Pt NPs can be preserved when treated at a lower temperature, the surface atoms of Pt NPs can be partially oxidized.[18] Additionally, the partial decomposition of PVP during the UV-O_3 process may result in other organic intermediates being adsorbed onto the surface of NPs, leading to deactivation of the catalyst.[19] The removal of capping agents from prepared NPs can also be accomplished with acid/based solutions. For example, acetic acid is used to remove oleylamine capping agent.[20] However, this treatment may leach out some metals (e.g. Pb) in Pt alloys when the solution is exposed to air.[13]

Recently, Zhang and coworkers have developed a universal method using an aqueous $NaBH_4$ solution to remove organothiols, hiophene, adenine, rhodamine, halide ions (Br^- and I^-) and PVP from Au nanoparticles.[21] Their computational studies indicate that these adsorbates can be displaced by hydride generated from $NaBH_4$ which has higher affinity to Au NPs than the adsorbates. However, the displaced capping agents can be re-adsorbed quickly onto the Au NPs with the depletion of $NaBH_4$.[21] Furthermore, the removal of capping agents from Pt or Pt alloy NPs using this method has not yet been reported. In this research, we have found that with assistance of tert-butylamine (TBA) $NaBH_4$ can completely remove PVP from the surface of Pt-Pd nanocubes (NCs) because the displaced PVP tends to be dissolved in the TBA solution to overcome re-adsorption issues. The modified method does not require a thermal treatment step so that the structure and shape of Pt-Pd NCs can be retained and the catalytic characteristics of the NCs preserved.

2. Experimental

2.1 Materials and Equipments

5% Nafion solution and sodium borohydride ($NaBH_4$) were purchased from Alfa Aesar. Tert-butylamine (TBA) and acetone and ethanol solvents were obtained from Sinopharm Chemical Reagent Co. Ltd. All other chemicals used in this research were purchased from Aladdin Industrial Inc. High purity water with 18.2 MΩ-cm resistivity was used throughout the experiments. UV-Visible spectrum measurements were taken using a Shimadzu UV-2550 spectrometer. TEM and high resolution TEM (HRTEM) images and the selected area energy dispersive spectra (EDS) were carried out using a JEM-2100 transmission electron microscope (TEM) (Link) equipped with a Link's EDS detector operated at 200 KV. X-ray diffraction (XRD) patterns were collected on a BRUKER-D8 X-ray diffractometer using Cu K-alpha radiation. Fourier transform infrared spectra (FTIR) were measured with a Nexus-870 infrared spectrometer. Raman spectra were acquired using a LabRAM HR Evolution Raman spectrometer operating at 532 nm.

2.2 Synthesis of Pt-Pd nanocubes

Pt-Pd alloy nanocubes (NCs) were synthesized following the procedure reported by Huang et al.[22] In detail, 1.0 mL of 20 mM Na_2PdCl_4 and 1.0 mL of 20 mM K_2PtCl_4 were dissolved in 10 mL

N,N-dimethylformamide (DMF). 0.5 mmol KI and 160.0 mg polyvinylpyrrolidone (PVP) were dissolved in the Pt-Pd precursor solution as the capping agents. After applying ultrasound for a few minutes the resulting homogeneous solution was placed in a 20 mL autoclave and heated at 130 ℃ for 5 hours. The product was then collected by centrifugation and washed four times with an ethanol/acetone solution. The obtained powder was labeled as "untreated Pt-Pd NCs".

2.3 PVP Removal

The removal of capping agent PVP from the surface of untreated Pt-Pd NCs was carried out using a $NaBH_4$/TBA aqueous solution. In a typical process, 6 mg as-prepared Pt-Pd NCs were treated in 25 mL $NaBH_4$/TBA aqueous solution ($NaBH_4$: TBA : H_2O = 1.9 mg : 20 mL : 5 mL) with stirring for 30 minutes at room temperature. After treatment the Pt-Pd NC sample was collected by centrifugation at 8000 rpm for 10 minutes. The collected sample was then washed three times with an ethanol/acetone solution to remove the excess surface-adsorbed amine. For comparison of PVP removal efficiencies, the untreated Pt-Pd NC samples were also treated separately with a pure TBA solution and an aqueous $NaBH_4$ solution using identical experimental procedures.

2.4 Kinetics of PVP desorption

Kinetics of PVP desorption from the surface of Pt-Pd NCs were measured using a time resolved UV-Vis spectrometer. The method is similar to that reported by Zhang et al.[21] First, 6.0 mg of the untreated Pt-Pd NCs were dispersed in 10.0 mL H_2O and sonicated for a few minutes. Then 0.30 mL of sonicated Pt-Pd NCs in water was transferred into a quart curette for kinetic measurements. After that, 1.80 mL TBA and 0.78 mL H_2O were added into the curette to form a homogeneous suspending solution. Finally, freshly prepared 0.05 M $NaBH_4$ (0.12 mL) in cold water was added to the solution, followed by immediate acquisition of time-resolved UV-Vis spectral measurements. Immediate and complete PVP desorption was observed upon $NaBH_4$ addition. For comparison, the kinetics of PVP desorption using either TBA or $NaBH_4$ solution were also carried out under the identical conditions.

2.5 Electrochemical measurements

The electrochemical measurements were performed using a CHI 660E Electrochemical Analyzer in a standard three-electrode cell. Working electrodes were prepared by dropping 5 μL prepared colloidal Pt-Pd cubic nanoparticles onto a glassy carbon electrode (GCE, 0.07 cm^2). A saturated calomel electrode (SCE) and a large Pt foil were used as the reference electrode and the counter electrode, respectively. Cyclic voltammetry (CV) was collected in a fresh 0.1 M $HClO_4$/1.0 M CH_3OH solution at a scan rate of 50 mV/sec. The potential range was 0.15 to 0.95 V (vs. SCE).

2.6 Photocatalytic activity measurements

The prepared Pt-Pd NCs were loaded onto CdS photocatalyst surface by an adsorption method introduced in electro-catalysis.[8, 23] The complete deposition of Pt-Pd nanoparticles onto CdS was confirmed by UV-Vis adsorption spectra previously introduced.[24] Visible light photocatalytic hydrogen production was carried out as follows: 0.05 g prepared Pt-Pd NCs/CdS powder was suspended in a 100 mL 1.0 M aqueous $(NH_4)_2SO_3$ solution. The solution was then transferred to a pyrex glass reactor cell (Perfectlight Co., Labsolar-I). The system was vacuum-degassed and irradiated using a 300W Xe lamp (PLS-SXE300/300UV, Perfectlight Co.). A water filter was used to remove the infrared light portion of the spectra and an optical cutoff filter to eliminate the UV radiation (< 420 nm). Hydrogen evolution was measured using an online gas chromatograph (Techcomp Limited Co., GC7890II) equipped with a thermal conductivity detector.

3. Results and discussion

3.1 Characterization of PVP removal from Pt-Pd nanocubes

Figure 1A shows typical TEM and high-resolution TEM (HRTEM) images of Pt-Pd alloy NCs. Counting over 200 nanoparticles in different regions of the sample, the average edge length of particles is 8.5 ± 0.2 nm with over a 93% yield for the cubic particles. The corresponding size distribution histogram and the HRTEM image are shown in the insets in Figure 1A. The result indicates that the Pt-Pd NCs are single crystals and enclosed by six {100} crystal planes. The distance from the two nearest fringes was measured to be 0.19 nm, close to the lattice spacing of 0.196 nm of {200} planes for the face-centered cubic (fcc) Pt crystal. Energy dispersive spectroscopic (EDS) analysis shows that both Pt and Pd are found in the nanoparticles (Supporting information, Figure S1). The TEM images for Pt-Pd NCs treated by $NaBH_4$/TBA, TBA and $NaBH_4$ are presented in Figure 1(B) - (D), respectively. The TEM images confirm that the shape or size of Pt-Pd NCs remain the same after cleaning with $NaBH_4$ and/or TBA. The crystalline structure of the NPs was further confirmed by the X-ray diffraction patterns (Supporting information, Figure S2), showing no significant changes before and after the $NaBH_4$/TBA treatment. These results all suggest that the novel treatment process for PVP removal from Pt-Pd

NPs does not affect the shape, size and crystallinity of the prepared particles.

The Raman spectra of untreated and $NaBH_4$/TBA treated Pt-Pd NCs solid samples are shown in Figure 2. As a reference, the spectrum of pure PVP powders is also measured under identical conditions. The obtained Raman spectra of pure PVP match well with previously measured PVP spectrum determined with laser excitation at 244 nm[25] and 632.8 nm.[26] However, Figure 2 shows significant differences between the Raman spectra of pure PVP and PVP-capped Pt-Pd NCs. The less intense and not well defined PVP peaks appeared in the Raman spectra of the PVP-capped Pt-Pd NCs are attributed to the resonance Raman Effect and the surface chemical enhancement effect.[25] These two factors make the amide groups in PVP more sensitive probes for the detection of interaction between PVP and metal nanoparticles. The intense bands at 1580 and 1360 cm^{-1} for the Raman spectrum of the PVP-capped Pt-Pd NCs are attributed to C=O stretch and CH_2 band modes of the pyrrolidone ring in PVP, respectively.[25] It is noted that the strength of characteristic peaks for PVP (C=O and CH_2 bend vibrational modes) on the surface of Pt-Pd NCs is in the order of: untreated NCs > TBA treated NCs > $NaBH_4$ treated NCs > $NaBH_4$/TBA treated NCs (Figure 2). This order suggests that after $NaBH_4$/TBA treatment the excess PVP could be completely removed from the surface of Pt-Pd NCs.

FTIR measurements further verify the complete removal of Pt-Pd NCs after $NaBH_4$/TBA treatment. Figure 3 shows the FTIR spectra of the untreated Pt-Pd NCs and $NaBH_4$/TBA treated Pt-Pd NCs. As a reference, the FT-IR spectrum of pure PVP powders was also included. (Figure 3(e)). The frequency of the characteristic vibrational modes of PVP matches well with those reported in the literature.[27-29] Unlike the Raman spectrum, the FTIR spectrum of PVP content Pt-Pd NCs is very similar to the pure PVP spectrum because only a small amount of pyrrolidone rings are able to interact with the metal surface.[25] As shown in Figure 3, the transmittance strength of PVP characteristic peaks (C=O; C-H_2; C-H and C-N) on Pt-Pd NCs decrease from untreated Pt-Pd NCs to TBA treated NCs to $NaBH_4$ treated NCs and to $NaBH_4$/TBA treated NCs. After $NaBH_4$/TAB treatment, only a trace amount of PVP remains on the surface of Pt-Pd NCs.

3.2 Effect of PVP removal on the catalytic activities of Pt-Pd NCs and Pt-Pd NCs/CdS

The electrochemical catalytic performances of the untreated and $NaBH_4$/TBA treated Pt-Pd NCs were carried out in a three-electrode system using a 0.1 M $HClO_4$ and 1.0 M CH_3OH aqueous electrolyte under Ar protection at room temperature (Figure 4). All potentials of the CV measurements were converted to the potentials of saturated calomel electrode (SCE). No electrical catalytic activity for methanol electrochemical oxidation was detected for untreated Pd-Pd NCs. This result suggests that the surface of the Pt-Pd NCs was completely covered with PVP and thereby blocked the access of electrolyte. Because of the strong interaction between PVP and Pt-Pd, TBA treatment can only partially remove PVP from the Pt-Pd surface under the present experimental conditions. Compared with untreated Pt-Pd NCs, the electrochemical activity of TBA treated Pt-Pd NCs improved insignificantly. Clearly enhanced activities for methanol oxidation were observed for the Pt-Pd NCs samples treated with $NaBH_4$ and $NaBH_4$/TBA. The peak current densities, J_f, in the forward scan are 17.0, 10.0 and 0.2 mA/cm^2 for $NaBH_4$/TBA, $NaBH_4$ and TBA treated Pt-Pd NCs, respectively. The order of the electrocatalytic activities of Pt-Pd NCs for methanol oxidation follows the reverse sequence of PVP adsorption strength in Raman and FTIR spectra as: untreated NCs < TBA treated NCs < $NaBH_4$ treated NCs < $NaBH_4$/TBA treated NCs. This result proves that the surface concentrations of PVP capping agent on Pt-Pd NCs are key factors determining the catalytic activity of Pt-Pd NCs. The highest electrocatalytic activity of Pt-Pd NCs sample treated with $NaBH_4$/TBA shows that $NaBH_4$/TBA treatment can effectively remove PVP from the surface of Pt-Pd NCs, leading to the highest activity.

PVP removal also strongly affects the photocatalytic activities of Pt-Pd NCs loaded CdS (Pt-Pd NCs/CdS) photocatalysts for H_2 production. As shown in Figure 5, untreated Pt-Pd NCs/CdS shows a low photocatalytic hydrogen production rate (359 μmol/h). In contrast, the rate of hydrogen production over $NaBH_4$/TBA treated Pt-Pd NCs/CdS increases to 1583 μmol/h under the same experimental condition (4.4 times increase). It is noteworthy that during a photocatalytic process proton reduction actually takes place on the surface of noble metal cocatalysts which are the active centers for hydrogen evolution. This greatly enhanced photocatalytic activity of treated Pt-Pd NCs/CdS indicates the importance of complete removal of PVP from Pt-Pd NPs. On the other hand, this result also indicates that the $NaBH_4$/TAB combined treatment method can effectively generate PVP free Pt-Pd NPs.

3.3 Mechanism of PVP removal from the surface of Pt-Pd nanocubes

Poly(N-vinyl-2-pyrrolidone) (PVP) is among the most commonly employed capping ligands in the size- and shape- controlled synthesis of metal nanocrystals. PVP can be chemically adsorbed onto the surface of metal nanocrystals with its oxygen atom or both the oxygen and nitrogen atoms in the ring of its molecule attaching to the metal d-orbitals. The adsorption process occurs rapidly in aqueous solutions. This was confirmed using UV-Visible adsorption spectra of metal colloidal solutions containing PVP. As shown in Figure 6A, the time-resolved UV-Visible absorbance spectrum revealed that the localized surface plasmon resonance (LSPR) absorbance of Pt-Pd NCs rapidly increases after the addition of PVP into a colloidal solution of Pt-Pd NCs. LSPR absorption spectrum is the characteristic light absorption property of a metal colloid. [30] It typically originates from the inter-band transitions of the metal nanoparticles. The evident increase in the Pt-Pd NCs LSPR absorbance peak after the PVP addition makes it possible to observe desorption and adsorption kinetics of PVP on Pt-Pd NCs. [21]

In contrast, slow desorption of PVP from the surface of Pt-Pd NCs was found when the PVP-capped Pt-Pd NCs was stirred in a TBA solution. As shown in Figure 6C, the Pt-Pd NCs LSPR absorbance slowly but continuous decreased in TBA solution. TBA is an organic solvent with high solubility for PVP and has been used to produce PVP free Pd NCs with a long time treatment.[29] Three days of TBA treatment are needed to produce PVP free metal NCs with the experimental condition (metal nanoparticles: TBA = 6 mg: 25 ml). However, although the rate is very slow, PVP capped on “the untreated” Pt-Pd NCs can be completely dissolved and restricted in TBA.

Rapid PVP desorption from Pt-Pd NCs can be achieved using $NaBH_4$. As shown in Figure 6B, an immediate decrease in Pt-Pd NCs LSPR absorbance is observed after the $NaBH_4$ addition into the PVP-capped Pt-Pd NCs colloidal solution. This result is attributed to that PVP adsorption on Pt-Pd competes with hydrides generated from $NaBH_4$ hydrolysis, which has stronger adsorption characteristics with metal nanoparticles than PVP.[21] Thus hydrides can displace PVP on the surface of Pt-Pd NPs. However, a gradual increase in the Pt-Pd NCs LSPR absorbance appeared with the increase of treatment time. This observation indicates that the surface-bound hydride is unstable and PVP can re-adsorb onto Pt-Pd NCs before the depletion of hydrides. The similar phenomenon had also been observed for PVP desorption and re-adsorption on Au NPS.[21] The rapid re-adsorption of PVP makes it difficult to obtain PVP free metal NPs using $NaBH_4$ treatment alone.

It is interesting to find that the re-adsorption of PVP is significantly minimized with TBA presence. As shown in Figure 6D, after a instant decrease after $NaBH_4$ addition, the Pt-Pd NCs LSPR absorbance continually decreased to the baseline level with the increase of treatment time and no PVP re-adsorption was observed. Based on the discussion above, the $NaBH_4$/TBA treatment method is caused by a combined effect of $NaBH_4$ and TBA. This integrated treatment process comprises of two steps and can be summarized as: (1) adsorbed PVP is displaced by the hydride generated from the hydrolysis of $NaBH_4$, resulting in the rapid desorption of PVP from Pt-Pd NCs. (2) the desorbed PVP is then dissolved and restricted in TBA. PVP re-adsorption was therefore eliminated even when the surface-bound hydride on Pt-Pd NCs was depleted.

4. Conclusions

PVP capping agent on the surface of Pt-Pd alloy nanocubes can be completely removed by using a modified $NaBH_4$ desorption method in the presence of TBA. HRTEM images and XRD patterns indicate that Pt-Pd NCs treated with $NaBH_4$ and/or TBA does not change the shape, size or crystallinity. The very low intensities C=O and CH_2 groups shown in Raman and FTIR suggest that the $NaBH_4$/TBA desorption method can efficiently remove PVP from the surface of shape-controlled Pt-Pd nanocubes under room conditions. As a comparison, $NaBH_4$- and TBA-treatment methods can only partially remove PVP from the surface of Pt-Pd nanocubes. This finding can be applied in the preparation of PVP free Pt and Pt alloy nanoparticles applicable for fuel cells, hydrogenation, photocatalysis and water electrolysis.

Acknowledgments

This work was financially supported by the National Natural Science Foundation of China (21103106, 21107069), Shanghai Key Project for Fundamental Research (13JC1402800), and the ‘‘Dawn’’ Program of Shanghai Education Commission (11SG52).

References

1. B. C. Steele and A. Heinzel, *Nature*, 2001, 414, 345-352.
2. H. Lee, S. E. Habas, S. Kweskin, D. Butcher, G. A. Somorjai and P. Yang, *Angewandte Chemie*, 2006, 45, 7824-7828.
3. K. M. Bratlie, H. Lee, K. Komvopoulos, P. Yang and G. A. Somorjai, *Nano letters*, 2007, 7, 3097-3101.
4. A. L. Linsebigler, G. Lu and J. T. Yates, *Chemical Reviews*, 1995, 95, 735-758.
5. V. R. Stamenkovic, B. S. Mun, M. Arenz, K. J. Mayrhofer, C. A. Lucas, G. Wang, P. N. Ross and N. M. Markovic, *Nature materials*, 2007, 6, 241-247.
6. J. Wu, A. Gross and H. Yang, *Nano letters*, 2011, 11, 798-802.
7. M. K. Carpenter, T. E. Moylan, R. S. Kukreja, M. H. Atwan and M. M. Tessema, *Journal of*

the American Chemical Society, 2012, 134, 8535-8542.

8. R. Narayanan and M. A. El-Sayed, *Nano letters*, 2004, 4, 1343-1348.
9. R. Narayanan and M. A. El-Sayed, *Journal of the American Chemical Society*, 2004, 126, 7194-7195.
10. N. Tian, Z. Y. Zhou, S. G. Sun, Y. Ding and Z. L. Wang, *Science*, 2007, 316, 732-735.
11. C. Wang, H. Daimon, T. Onodera, T. Koda and S. Sun, *Angewandte Chemie*, 2008, 47, 3588-3591.
12. J. A. Lopez-Sanchez, N. Dimitratos, C. Hammond, G. L. Brett, L. Kesavan, S. White, P. Miedziak, R. Tiruvalam, R. L. Jenkins, A. F. Carley, D. Knight, C. J. Kiely and G. J. Hutchings, *Nature chemistry*, 2011, 3, 551-556.
13. Z. Niu and Y. Li, *Chemistry of Materials*, 2014, 26, 72-83.
14. R. M. Rioux, H. Song, M. Grass, S. Habas, K. Niesz, J. D. Hoefelmeyer, P. Yang and G. A. Somorjai, *Topics in Catalysis*, 2006, 39, 167-174.
15. Z. L. Wang, J. M. Petroski, T. C. Green and M. A. El-Sayed, *The Journal of Physical Chemistry B*, 1998, 102, 6145-6151.
16. M. Comotti, W. C. Li, B. Spliethoff and F. Schuth, *Journal of the American Chemical Society*, 2006, 128, 917-924.
17. L. Menard, F. Xu, R. Nuzzo and J. Yang, *Journal of Catalysis*, 2006, 243, 64-73.
18. C. Aliaga, J. Y. Park, Y. Yamada, H. S. Lee, C.-K. Tsung, P. Yang and G. A. Somorjai, *The Journal of Physical Chemistry C*, 2009, 113, 6150-6155.
19. C. H. Bartholomew, *Applied Catalysis A: General*, 2001, 212, 17-60.
20. D. Li, C. Wang, D. Tripkovic, S. Sun, N. M. Markovic and V. R. Stamenkovic, *ACS Catalysis*, 2012, 2, 1358-1362.
21. S. M. Ansar, F. S. Ameer, W. Hu, S. Zou, C. U. Pittman, Jr. and D. Zhang, *Nano letters*, 2013, 13, 1226-1229.
22. X. Huang, Y. Li, Y. Li, H. Zhou, X. Duan and Y. Huang, *Nano letters*, 2012, 12, 4265-4270.
23. C. K. Tsung, J. N. Kuhn, W. Huang, C. Aliaga, L. I. Hung, G. A. Somorjai and P. Yang, *Journal of the American Chemical Society*, 2009, 131, 5816-5822.
24. W. Yao, C. Huang, N. Muradov and A. T-Raissi, *International Journal of Hydrogen Energy*, 2011, 36, 4710-4715.
25. Y. Borodko, S. E. Habas, M. Koebel, P. Yang, H. Frei and G. A. Somorjai, *The journal of physical chemistry. B*, 2006, 110, 23052-23059.
26. D. L. A. de Faria, H. A. C. Gil and A. A. A. de Queiróz, *Journal of Molecular Structure*, 1999, 478, 93-98.
27. J. Bai, Y. Li, C. Zhang, X. Liang and Q. Yang, *Colloids and Surfaces A: Physicochemical and Engineering Aspects*, 2008, 329, 165-168.
28. J. Xian, Q. Hua, Z. Jiang, Y. Ma and W. Huang, *Langmuir : the ACS journal of surfaces and colloids*, 2012, 28, 6736-6741.
29. N. Naresh, F. G. S. Wasim, B. P. Ladewig and M. Neergat, *Journal of Materials Chemistry A*, 2013, 1, 8553.
30. J. A. Creighton and D. G. Eadon, *Journal of the Chemical Society, Faraday Transactions*, 1991, 87, 3881.

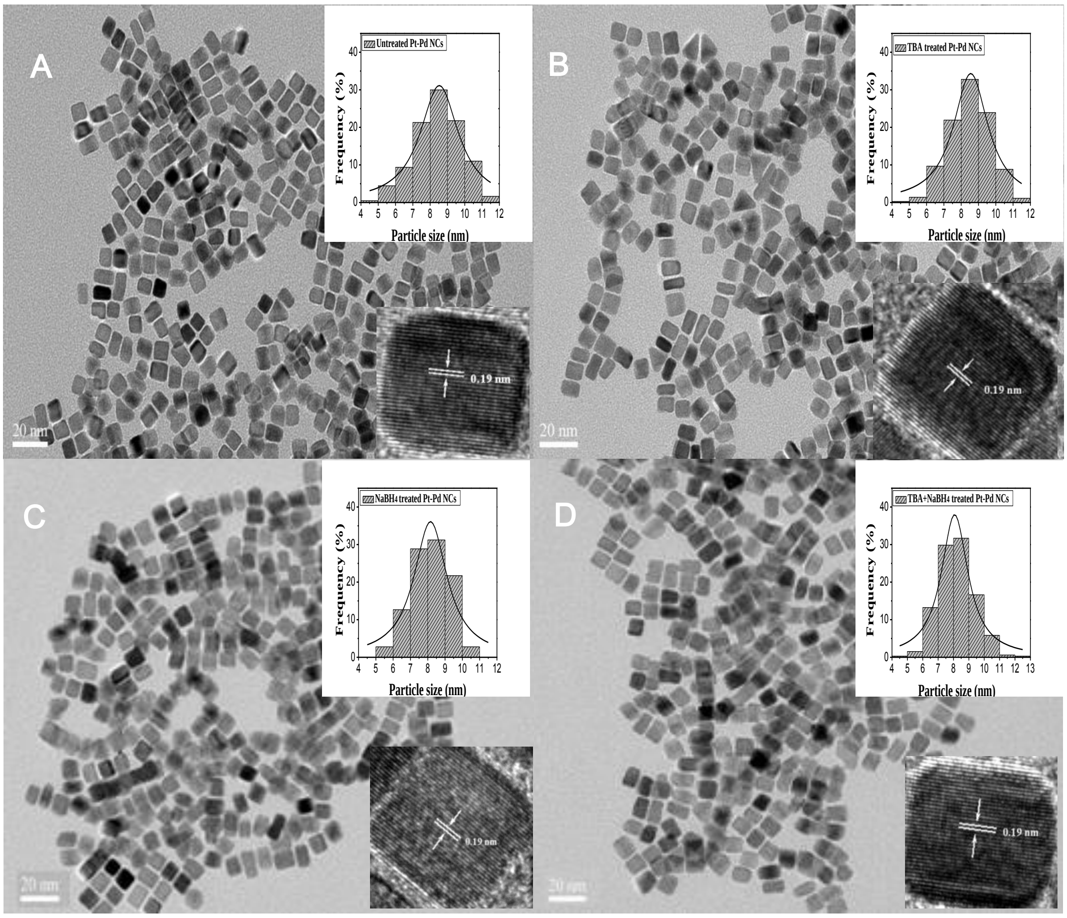

Figure 1. TEM images of the Pt-Pd alloy nanocubes: (A) untreated ; (B) TBA treated; (C) $NaBH_4$ treated and (D) TBA/$NaBH_4$ treated Pt-Pd nanocubes. Insets: High resolution images and particle size distributions of the Pt-Pd nanocubes. The lattice spacing of 0.19 nm can be indexed to the {200}reflection of Pt or Pd.

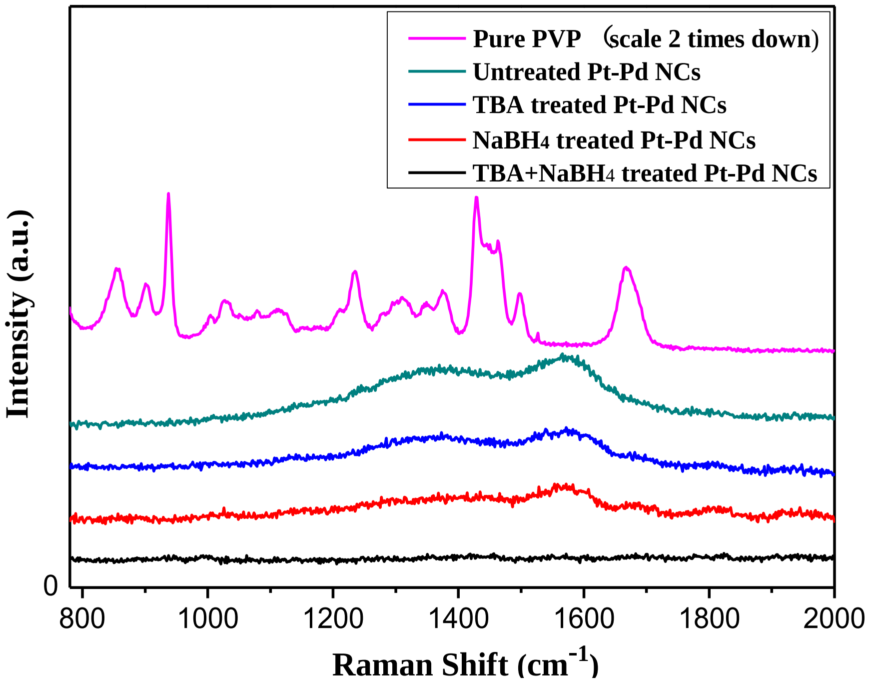

Figure 2. Raman Spectra of pure PVP powders and Pt-Pd alloy nanocubes samples with different treatment methods.

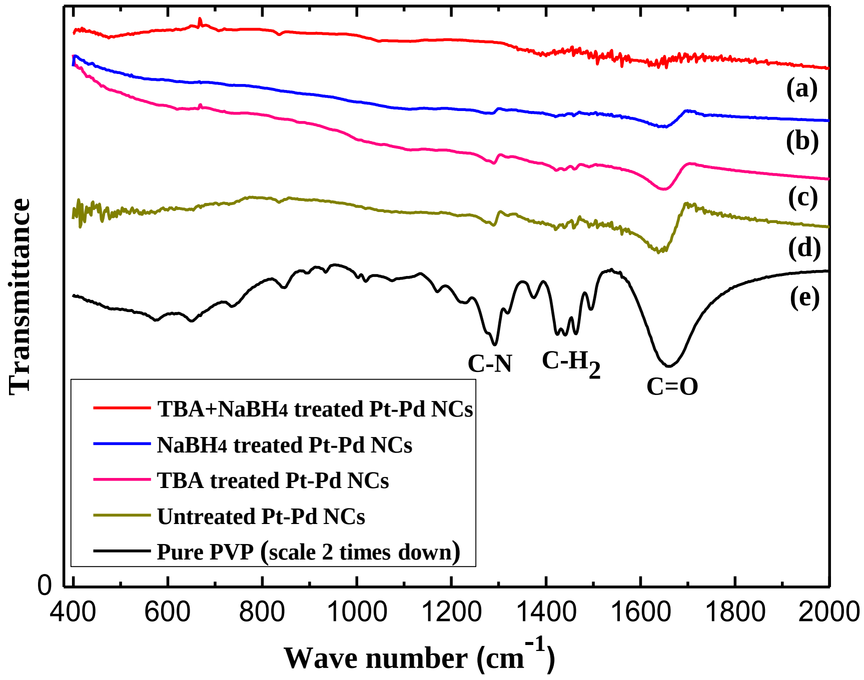

Figure 3. FTIR Spectra of PVP and the prepared Pt-Pd alloy nanocubes with various treatment methods.

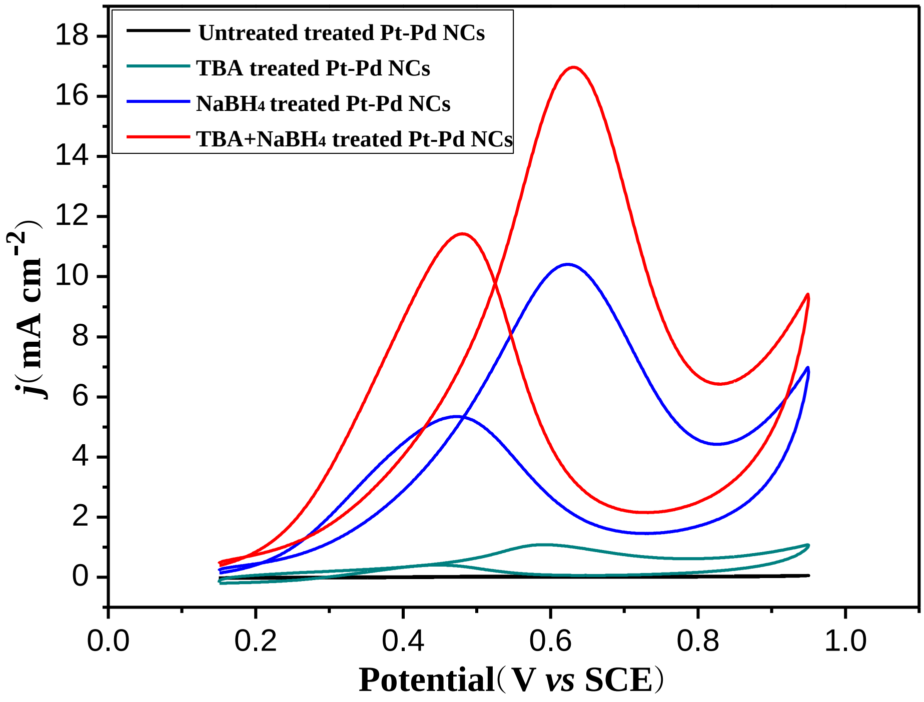

Figure 4. CV curves of the Pt-Pd nanocubes in a 0.1 M $HClO_4$/ 1.0 M CH_3OH aqueous solution at a scan rate of 50 mV s^{-1}

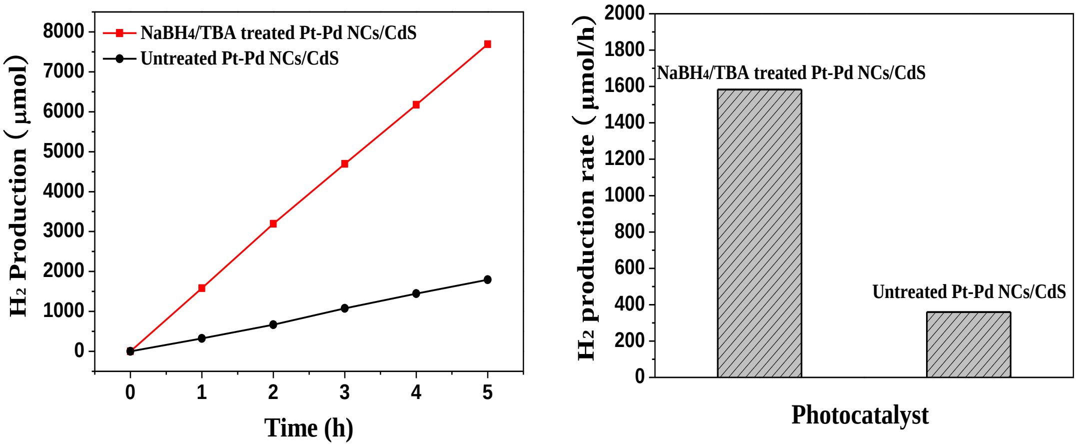

Figure 5. Photocatalytic activities of Pt-Pd NCs loaded CdS photocatalysts for hydrogen production under visible light irradiation. (a). Hydrogen production vs. time and (b) H_2 production rate. (CdS weight: 0.05 g, Pt-Pd NCs weight: 0.25 mg, photolyte: 1.0 M $(NH_4)_2SO_3$, Light Source: 300W Xe lamp equipped with a 420 nm optical cutoff filter).

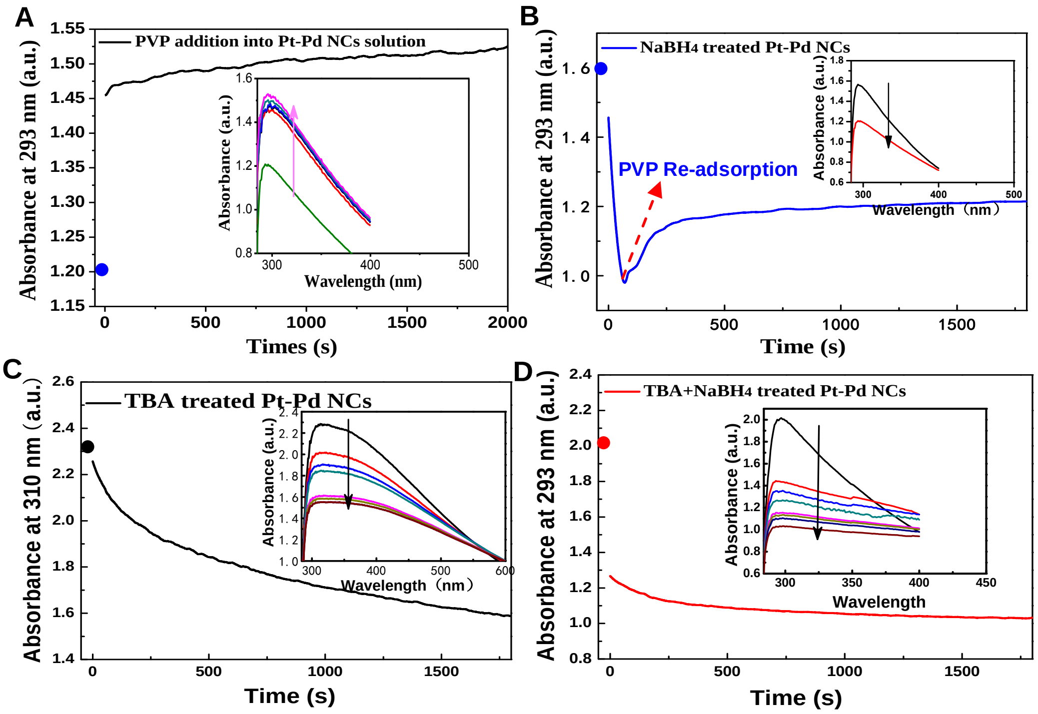

Figure 6 (A). Absorbance of localized surface plasmon resonance (LSPR) for Pt-Pd nanocubes in water after PVP addition; (B). LSPR absorbance of PVP-capped Pt-Pd NCs in water after $NaBH_4$ addition; (C). LSPR absorbance of PVP-capped Pt-Pd NCs in TBA. (D) LSPR absorbance of PVP-capped Pt-Pd NCs in TBA after $NaBH_4$ addition. The dots are the LSPR absorbance of colloidal Pt-Pd NCs before treatment. Insets: the time-resolved UV-Visble spectra of prepared Pt-Pd NCs samples. The arrows show the decrease of the absorbance with the increase of treatment time.

Table of contents entry

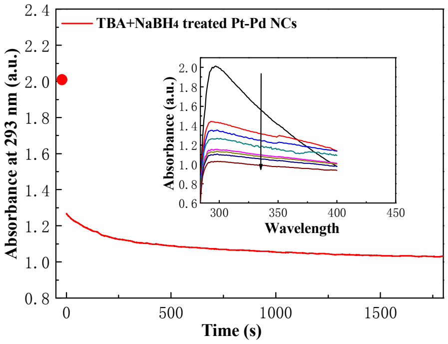

A facile $NaBH_4$/tert-butylamine (TBA) treatment method for the effective removal of PVP from Pt alloy nanoparticles without affecting particle morphology